



Water storage and redistribution effect evaporation, retention, and infiltration of forest floor sites

Heinke Paulsen¹, Markus Weiler¹

¹Chair for Hydrology, Albert Ludwig University, Freiburg, 79098, Germany

5 *Correspondence to:* Heinke Paulsen (Heinke.paulsen@hydrology.uni-freiburg.de)

Abstract. The forest floor (FF) possesses a significant water retention capacity, facilitating the transfer of water between the atmosphere and the soil. However, knowledge on the water retention characteristics and water redistribution effects of the FF remain limited. Due to the dominance of laboratory data regarding the storage capacity of a forest's litter layer, we used a combined FF weighted grid-lysimeter and soil moisture network to directly and in-situ measure the dynamics of water storage

10 of the FF and fluxes from and into the FF. The objective was to quantify storage capacities, retention durations, and resulting water redistribution patterns, as well as evaporation from the FF. We present the results of our network at three sites with different altitudes located in the Black Forest, southwest Germany. The three sites have an annual mean temperature gradient from 6.3°C to 10.3 °C, leading to humus forms that vary from typical F-Mull to typical Moder. Throughout the monitored period in 2024-2025, the storage capacity of the FF ranged between 1.4 and 4.2 g/g FF and was not only influenced by the
15 type of litter but also by the rainfall characteristics themselves. With our field setup we could show that longer, low intensity rainfall events fill the FF storage more efficiently than shorter heavy rainfall events (- 24 %). Our gridded lysimeter design revealed small-scale spatio-temporal infiltration patterns, caused by a redistribution of rainfall along the passage through the FF. The findings of the lysimeter network provide a comprehensive understanding of the influence of the FF mass on the water cycle within forest ecosystems.

20 1. Introduction

Understanding the partitioning and movement of water within temperate forest ecosystems is essential for predicting hydrological responses to changing environmental conditions. At the interface between the atmosphere and the soil, the forest floor (FF) litter layer serves as a critical mediator of water fluxes, influencing processes such as runoff generation, soil moisture refilling, and soil evaporation. Despite its relatively small thickness, this organic layer regulates the fate of precipitation before
25 it infiltrates the mineral soil, affecting both water availability and overall ecosystem functioning (Ilek et al., 2021).

The interception of rainfall by the FF plays a significant role in the water balance of forest soils. This layer, characterized by varying leaf structures and organic material, undergoes temporal compositional changes due to canopy phenological phases and disturbances (Van Stan et al., 2017). Just like variations in canopy thickness result in different initial throughfall amount (Nanko et al., 2022), FF substantially influences the amount of water available for soil infiltration and runoff (Guevara-Escobar



30 et al., 2007). But despite its importance, there is still relatively little data available on this phenomenon (Gerrits et al., 2007; Zagyvai-Kiss et al., 2019; Zhao et al., 2022).

During a typical rainfall event the FF shows different functions regarding the water cycle. *Initial rainfall retention* of litter refers to the capacity of the FF's layer of organic material—composed of leaves, twigs, and other decomposing plant matter—to temporarily hold or store rainfall at the onset of a rain event. This retention occurs before the water begins to infiltrate into 35 the mineral soil or contributes to runoff. With further rainfall the FF will store more water until it reaches the *maximum storage capacity* (C_{max}), also known as the interception capacity (Putuhena and Cordery, 1996). With ceasing rainfall and gravitational draining water leaving the FF it reaches the minimum storage capacity (C_{min}). The than stored water is only available for *evaporation*. Higher evaporation occurs immediately after a rainfall event from the FF (E_{FF}), whereas stable evaporation 3-4 days later primarily originates from the soil layer (Deguchi et al., 2008). Understanding these processes is essential to 40 accurately assess water balances in forest ecosystems.

The ability of FF to intercept and temporarily store precipitation is critically dependent on the physical characteristics of the FF as well as rainfall conditions (Li et al., 2020). Lysimeter studies offer an accurate means to quantify flux and storage processes (Levia et al., 2011). It has been observed that broadleaf litter has a larger interception capacity than needle litter, attributed to its higher surface area-to-weight ratio (Walsh and Voigt, 1977; Zhao et al., 2022). Structural differences in the 45 litter layer lead to heterogeneous flow patterns, with water preferentially following in defined paths, leaving portions of the lower litter unwetted (Walsh and Voigt, 1977).

Post-rainfall grab sample observations reveal that the FF's ability to store and evaporate water is highly dependent on its thickness, pre-wetness condition, and the intensity and duration of rainfall. In natural rainfall conditions, interception storage capacities change with rainfall intensity and litter types due to differences in the morphological characteristics of litter flow 50 pathways (Sato et al., 2004). Notably, the litter layer can retain and cycle up to 18% of annual precipitation or approximately one-third of annual evapotranspiration (Floriantic et al., 2023). Although FF surfaces can store only a few millimetres of water, their impact becomes significant over longer time scales as the storage is frequently filled and depleted (evaporated) due to the high frequency of small rainfall events, thereby reducing soil moisture recharge and runoff generation (Levia et al., 2011). The importance of retention and storage capacity in maintaining forest hydrology cannot be overstated. Evaporation from a 55 broadleaf FF can reach rates of around 0.2 ± 0.13 mm/day in a humid subtropical climate, with significant seasonal variations (Deguchi et al., 2008). While Magliano et al. (2017) found considerably higher first day evaporation to be 1.1 ± 0.3 mm/day also in a humid subtropical climate for forest litter.

This study aims to test the following hypotheses: (1) thicker FF results in higher initial rainfall retention, depending on initial 60 wetness conditions, (2) thicker FF leads to higher total water storage capacities, (3) infiltration is heterogeneous on a small spatial scale, influenced not only by the spatially variable incoming canopy throughfall but enhanced by lateral redistribution of water in the FF, and (4) thicker FFs function as a barrier for evaporation from the mineral soil. To test all these hypotheses, we established an extensive FF lysimeter network, installed at three different sites throughout the Black Forest SW Germany.



2. Methods

65 2.1. Sites

This study utilizes a network of novel forest floor lysimeters (Paulsen and Weiler, 2025) and soil moisture probes deployed across three mixed forest sites with the main species being beech (*Fagus sylvatica*) and spruce (*Picea abies*). The sites are situated at different altitudes in the Black Forest region of southwestern Germany. These sites have an annual mean temperature gradient ranging from 6.3°C to 10.3°C and a mean annual precipitation gradient between 1100 and 1770 mm, which results in
70 varying humus forms from typical F-Mull to typical Moder, classified according to the KA6 system (AG Boden, 2024).
Additional information regarding the characteristics of these sites can be found in Table 1.

Table 1: Detailed characteristics of the three research sites in the Black forest, Germany.

	Waldkirch	Conventwald	Kandel
Altitude (m.a.s.l)	415	841	1163
Mean annual temperature (1991-2020)	10.3 °C	7.8 °C	6.3 °C
Mean annual precipitation (1991-2020)	1107 mm	1459 mm	1769 mm
Humus Form ¹	Typical F-mull	Typical Moder	Typical Moder
FF thickness*	5.5 cm	8.5 cm	8.1 cm
FF mass*	0.82 kg/m ²	3.66 kg/m ²	5.03 kg/m ²
Soil type ²	Dystric Cambisol (pantoloamic, ochric, endostagnic)	Dystric skeletal Cambisol (pantoloamic, folic, humic)	Dystric skeletal Cambisol (pantoloamic, ochric, epiraptic)
Bedrock	Gneis	Paragneis	Gneis

¹ KA 6 (AG Boden, 2024), ² WRB 4th Ed. (International Union of Soil Sciences, 2022), *sampling in autumn 2023



75 **2.2. Installations**

At each of the three sites, we installed four weighted forest floor grid lysimeters (FFGL) in September/October 2023. The FFGLs were designed to generate data with high temporal resolution across multiple locations and varying spatial scales (Paulsen and Weiler, 2025). Therefore, a low-cost setup to install multiple lysimeters at several study sites was necessary. Figure 1a illustrates the FFGL, comprising a weighted container containing the FFs organic layer and top mineral soil, and a frame supporting the measurement equipment, like load cells and tipping buckets, and securing the system in the soil. The FFGL containers with a surface area of 25 x 100 cm were filled with the upper 15 cm of material from the surface, accommodating litterfall in autumn. To explore the small-scale heterogeneity of infiltration patterns, the lysimeter bottom was partitioned into four grids (each 0.0625 m²), facilitating a typical grid lysimeter approach that enables the observation of outflow from each grid with a tipping bucket independently. A detailed description of the FFGL is provided in (Paulsen and Weiler, 2025). Each lysimeter is coupled with two soil moisture probes (SMT100, Truebner GmbH, Germany), positioned 50 cm adjacent to the lysimeter at two depths below the soil surface (5 cm and 15 cm), as depicted in Figure 1. Additionally, microclimate parameters below the canopy, including air temperature, humidity, and radiation, were recorded at each site using two small meteorological stations (SnoMos, Pohl and Garvelmann (2015)). To obtain a representative mean for each site, the lysimeters were strategically positioned relative to the two tree species beech (*Fagus sylvatica*) and spruce (*Picea abies*): one was placed beneath the crown edge, and the other was situated halfway between the crown edge and the tree stem.

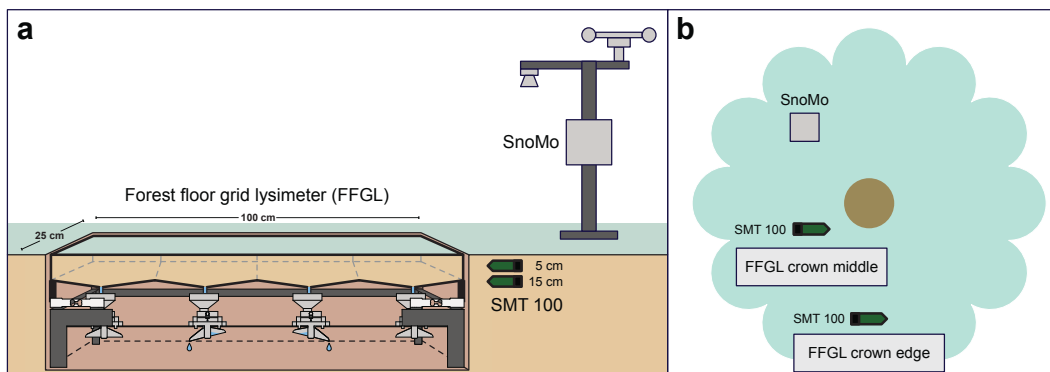


Figure 1: Installed setup (a) containing a microclimate station (SnoMo), soil moisture probes (SMT100) and forest floor grid lysimeters (FFGL), and (b) the corresponding positioning to the tree.

Since storage processes should be related to a certain dry mass of FF, we disentangled the lysimeters after almost two years in summer 2025, oven dried and weighed the material. The results are depicted in Table 2.



100 **Table 2: Oven dry weight of lysimeter fillings (area = 0.25 m²), separated in FF and mineral soil.**

Site	Position	Weight (kg)		
		FF	Mineral soil	Total
Waldkirch	Beech CE	0.76	19.7	20.5
	Beech CM	0.97	16.8	17.8
	Spruce CE	0.68	18.5	19.2
	Spruce CM	0.75	24.4	25.1
Conventwald	Beech CE	1.15	9.3	10.5
	Beech CM	1.11	10.6	11.7
	Spruce CE	0.75	6.8	7.6
	Spruce CM	0.43	9.2	9.6
Kandel	Beech CE	2.33	7.4	9.7
	Beech CM	2.04	9.9	11.9
	Spruce CE	2.61	4.6	7.2
	Spruce CM	1.29	5.6	7.9

CE = crown edge, CM = crown middle

2.3. Data processing

Forest floor grid lysimeter

105 The lysimeters microcontroller was programmed to measure the container weight with four load cells and number of tips for each of the four tipping buckets in a 10-minute time step. We here present the data collected from Mai 2024 to August 2025. These measurements of the weighing FFGL can be used to determine the water balance of the FF for each observed time step. The amount of water percolating to the deeper soil D can be determined by multiplying the number of tipping bucket tips n with the specific tipping volume. This specific tipping volume was determined by calibration with 250 ml water in the field.

110 With an average tipping volume of 2.1 ml and the area covered by each lysimeter grid (0.0625 m²), we reach a resolution of 0.03 mm for the draining water. The load cells continuously measure the storage mass S and, consequently, the mass of the lysimeter. If there is no drainage and the weight change is negative, we assume that this change is due to evaporation E from the FF.



115

$$\text{If } D = 0 \& \Delta S < 0$$

$$E = \Delta S$$

(1)

120

$$P_{TF} = E + D + \Delta S$$

(2)

Event analysis

125 Figure 2 shows a schematic representation of an exemplary precipitation event. The event can be divided into several typical phases. The first phase, termed the *initial rainfall retention* phase, is characterized by the lysimeter gaining weight without any drainage occurring. In the subsequent phase, the lysimeter continues to gain weight until it reaches its maximum storage capacity (C_{\max}), known as the FF interception capacity. During this phase drainage from the lysimeter begins. As the rainfall ends, the weight of the lysimeter decreases due to ongoing drainage. Once drainage stops, the FF reaches C_{\min} , representing 130 the minimum storage capacity or its water holding capacity. The water retained at this point can only be further depleted through evaporation (Putuhena and Cordery, 1996).

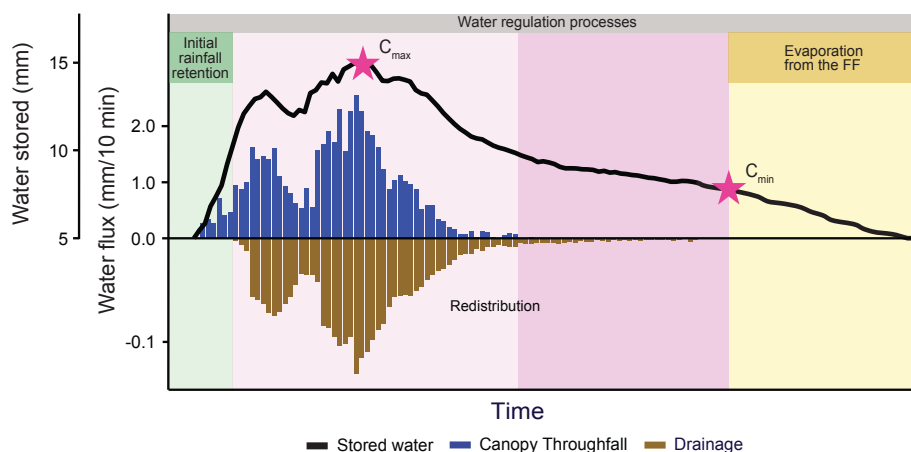


Figure 2: Exemplary run of one precipitation event, including precipitation and drainage amount as well as the progression of lysimeter weight, showing the different phases initial rainfall retention, storage, redistribution and evaporation.



135 To analyze different types of precipitation events, we first established a clear definition of an event. For our purposes, an event
is characterized by a positive storage increase exceeding 0.02 mm for more than three consecutive time steps, thus ensuring
that isolated increases in weight (e.g., due to falling branches, needles or leaves) are not mistakenly classified as precipitation.
An event is considered to have ended when there are 36 consecutive time steps (equivalent to 6 hours) without a positive water
flux. Additionally, the total precipitation amount for the event must exceed 0.5 mm. With these criteria, we were able to
140 identify events of varying sizes, intensities and durations.

Initial rainfall retention: We assessed the time lag between throughfall and drainage for different events, determining the
period during which the FF can retain incoming water before it percolates to deeper soil layers, and examined the duration of
this retention. We correlated retention sum and time to the initial soil moisture content for these events. We hypothesize that
longer retention times would correspond to drier initial conditions. This relationship was tested for statistical significance.

145 **Storage capacity:** We can identify two different storage capacities of the FF (Putuhena and Cordery, 1996). The first one
represents the minimum interception storage capacity (C_{\min}) of the litter layer. This is defined as the amount of water retained
in the litter layer when free drainage ceases after rainfall. C_{\min} is comparable to the water holding capacity concept used in soil
sciences for describing storage in porous media. It excludes gravitational water and is depleted solely by evaporation. In
contrast C_{\max} is referred to as the FF interception capacity, which can also be defined as (C_{\max}) the maximum interception
150 storage capacity of the FF, taken as the amount of water retained in the FF when the litter interception stops increasing during
rainfall. It includes gravitational water.

Evaporation: Given that evaporation is a relatively slow and gradual process, we analyzed it using hourly data. During dry
periods (i.e., intervals without rain events), we examined the hourly changes in weight. After accounting for drainage, the
decrease in weight can be attributed to evaporation.

155 **Infiltration Redistribution:** By not only measuring the total weight of the lysimeter box but also recording the weight at each
individual load cell at the corner of the rectangular container (Paulsen and Weiler, 2025), we are able to deduce the spatial
distribution of canopy throughfall across the lysimeter surface. While we cannot provide absolute values, this approach still
allows us to determine whether precipitation is preferentially reaching the surface at the left or right side of the lysimeter box,
or if it is distributed relatively evenly across the surface. The gridded lysimeter bottom with its corresponding tipping bucket
160 counts, allows us for direct observation of the spatial distribution of drainage.

3. Results

3.1. Water fluxes

The FFGLs allow for detailed determination of the water fluxes into and from the FF. In Figure 3 we show the absolute hourly
water fluxes of one selected exemplary event during the observed time period including the corresponding cumulative water
165 fluxes for all twelve studied lysimeters.

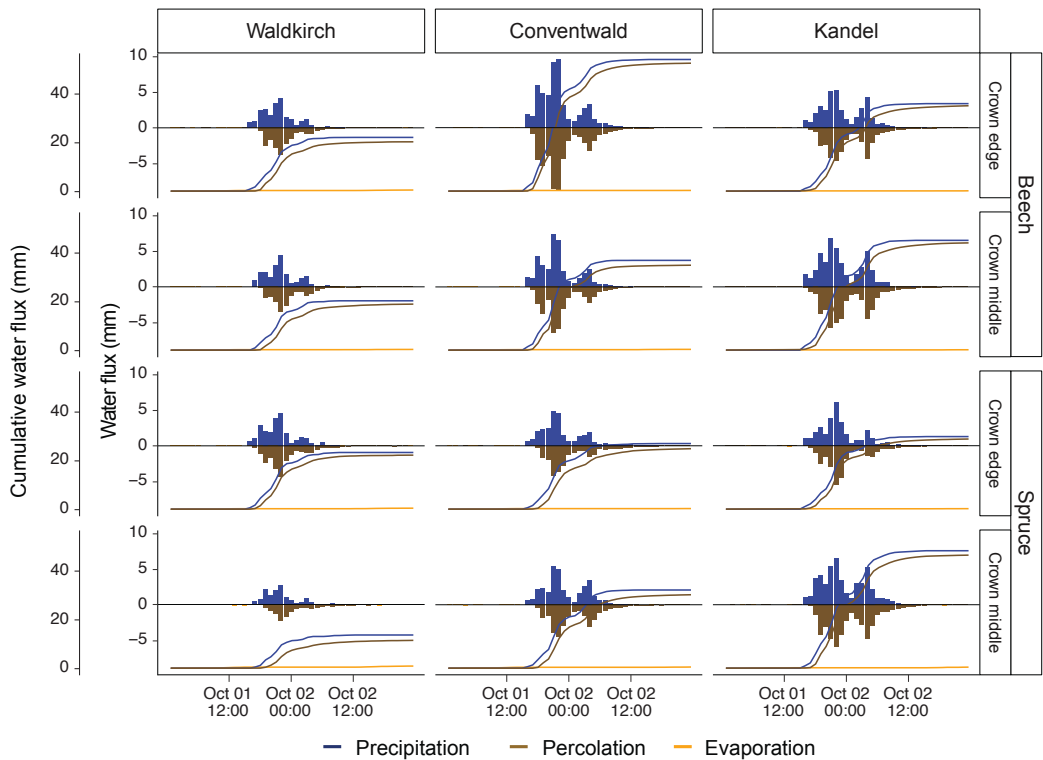


Figure 3: Total and cumulative hourly water fluxes of precipitation, percolation and evaporation for a selected rainfall event in fall 2024 (1.10.2024).

According to the different sites with their different altitudes, we see the highest precipitation amount on Kandel and slightly lower on Conventwald and much lower in Waldkirch (Table 3). Comparing the different locations under the trees it becomes evident that there are differences in canopy throughfall amount but the relation between throughfall and drainage is quite similar for all lysimeters.



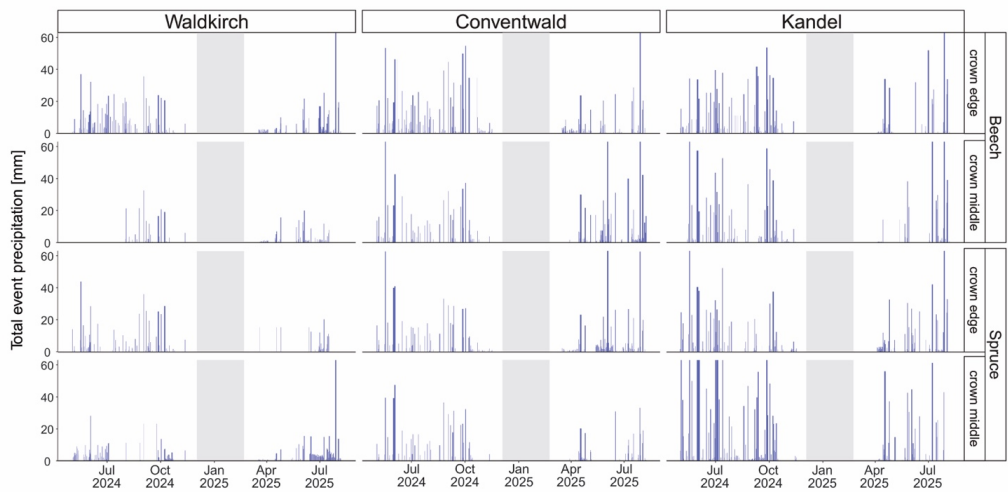
Table 3: Total mean amount of fluxes during the selected event 1.10.2024.

Location		P_{TF} (mm)	Drainage (mm)	Evaporation (mm)
Waldkirch	Beech CE	22.0	20.2	0.5
	Beech CM	20.2	18.9	0.3
	Spruce CE	23.2	22.1	0.4
	Spruce CM	13.6	11.4	0.9
	Mean	19.8	18.2	0.5
Conventwald	Beech CE	54.0	52.4	0.3
	Beech CM	36.8	34.8	0.3
	Spruce CE	26.9	24.8	0.3
	Spruce CM	32.1	30.1	0.5
	Mean	37.4	35.5	0.3
Kandel	Beech CE	35.9	35.0	0.1
	Beech CM	45.0	44.0	0.2
	Spruce CE	29.8	28.8	0.2
	Spruce CM	48.2	46.4	0.4
	Mean	39.7	38.5	0.2

CE = crown edge, CM = crown middle

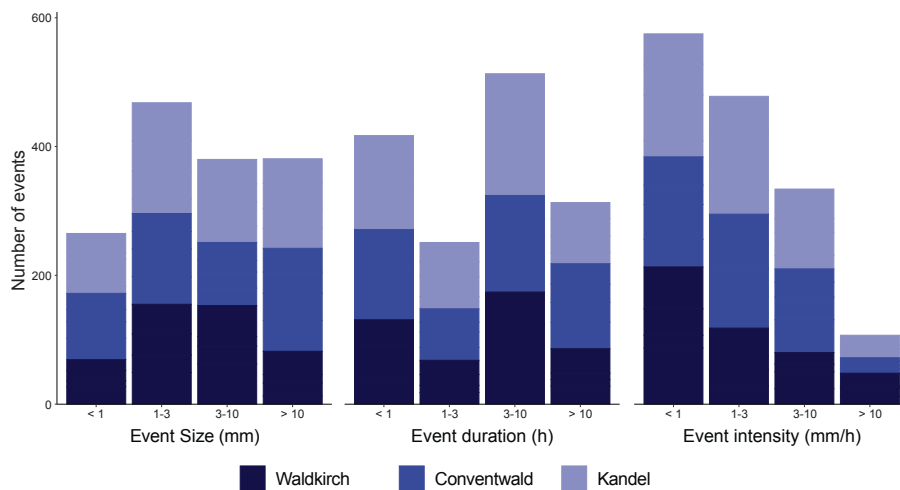
3.2. Precipitation events - identification

180 In total, we identified 1,570 precipitation events from May 2024 to July 2025 across the three locations and differently positioned lysimeters (in average over 130 events per lysimeter). The winter period (November to February) was excluded from the analysis as frequently precipitation during this time involved snowfall and related snowmelt periods, which cannot be accurately measured with the lysimeters alone. The temporal resolution, including the duration and timing of the identified events (Figure 4), was consistent among the lysimeters at each site, and the measured intensities were also comparable. We
 185 recorded the highest number of events ($n = 551$) in Conventwald. At the other two sites, we identified 511 events in Waldkirch and 508 events in Kandel. The number of events recorded by individual lysimeters varied, ranging from 91 to 172 events. Differences in the total numbers are caused by data gaps in single lysimeters due to various technical difficulties.



190 **Figure 4: Identified rainfall events and their total P_{TF} for all twelve lysimeters, the snow-affected period which was excluded from the statistical analysis is rendered in grey.**

For a characterization of these events, we analyzed their size, intensity, and duration. Figure 5 illustrates the distribution of these characteristics. To highlight some specific cases: 18% of the events are very small, ranging between 0.5 and 1 mm, whereas 25% exhibit a total precipitation amount exceeding 10 mm. The majority of events (70%) show average rainfall intensities below 3 mm/h, with only 7% experiencing intensities greater than 10 mm/h. The duration distribution presents a 195 slightly different pattern, with a substantial portion of events lasting less than one hour (28%) and another high portion between 3 and 10 hours (33%). Only 17% of the events last between one and three hours, and 21% exceed a duration of 10 hours. Notably, we also identified 83 events that lasted longer than 24 hours.



200 **Figure 5: Measured size, intensity and duration of the observed events.**

3.3. Retention and moisture content

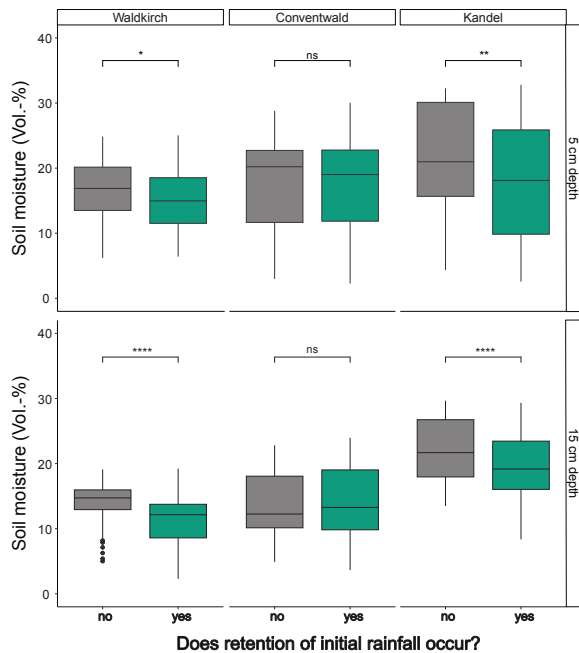
Approximately 72% of the observed precipitation events showed retention of water in the FF for periods exceeding 10 minutes. The average amount of initially retained rainfall water varied, ranging from 0.23 g/g FF at the Kandel site to 0.15 g/g mm at the Waldkirch site (Table 4). The maximum retained precipitation amounts before drainage started was detected between 1.08 g/g at Waldkirch and 1.22 g/g at Kandel. In terms of duration, the longest retention times were recorded at the Waldkirch site. Notably, the volume of retained water tended to increase with higher precipitation totals.

Table 4: Initial rainfall retention statistics for the three research sites.

Location	Mean	water	Max	water	Mean retained time
	retention		retention		(h)
	(g/g)		(g/g)		
Waldkirch	0.15		1.08		6.5
Conventwald	0.23		1.70		3.5
Kandel	0.19		1.22		2.7



210 Given the absence of significant differences in retention amounts and durations among the three sites, we investigated other potential influencing factors, such as pre-event soil moisture. Our findings indicate that pre-event soil moisture significantly affects the likelihood of initial rainfall retention (duration > 10 minutes) at Conventwald and Kandel site. Figure 6 illustrates the comparison of relative soil moistures for events with and without retention, revealing a tendency for retention to occur at lower soil moisture levels.



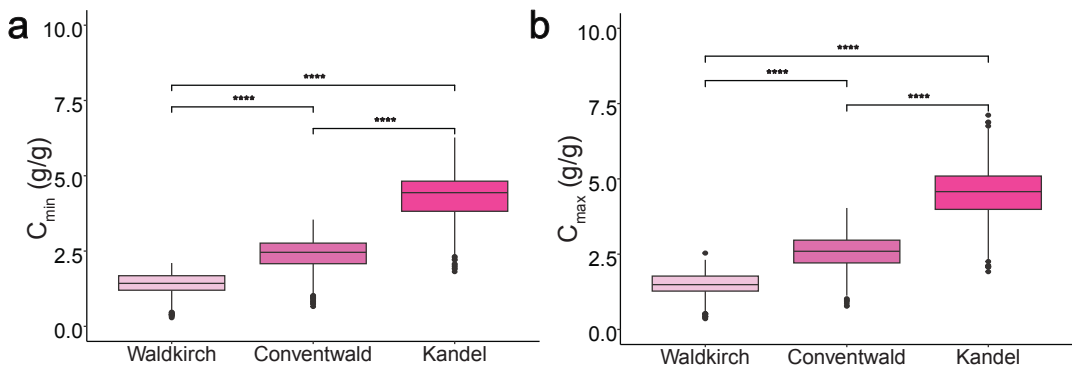
215

Figure 6: Tendency for retention to occur in relation to soil moisture at 5 and 15 cm depth. We found a significant difference in soil moisture leading to initial rainfall retention or not in Waldkirch and at Kandel. Overlaid significance symbols indicate the results of statistical t-tests between the groups. The significance levels are represented as follows: *($p \leq 0.05$), **($p \leq 0.01$), *($p \leq 0.001$), ****($p \leq 0.0001$), and ns ($p > 0.05$)**

220

3.4. Storage capacity

The mean water holding capacity (C_{min}) of the FF exhibits high variation across the three sites (Figure 7a), ranging from 1.4 g/g FF in Waldkirch and 4.2 g/g at Kandel. A statistically significant difference in the mean C_{min} values is observed between all sites. The pattern observed for interception capacity (C_{max}), which corresponds to short-term storage (Figure 7b), resembles 225 that of C_{min} , but is higher since gravitational water is included. The mean interception capacity ranges from 1.5 g/g at the Waldkirch site to 4.4 mm at Kandel. Once again, Conventwald and Kandel exhibit higher values at a similar level, suitable to their similar FF characteristics (typical Moder). The interception capacity for all sites differs significantly.



230 **Figure 7: Mean water holding capacity (C_{min}) on the three different research sites and for different precipitation durations. Overlaid**
significance symbols indicate the results of statistical t-tests between the sites. The significance levels are represented as follows:
231 ******(p ≤ 0.0001).**

232 The water holding capacity (C_{min}) is significantly influenced by the duration and, consequently, the intensity of rainfall events
233 (Figure 8a). Longer event durations, typically associated with lower intensities (Figure 8b), allow for more effective filling of
the storage capacity, resulting in an increase in C_{min} with extended rainfall durations. Conversely, during higher intensity events,
234 water tends to flow rapidly through the relatively large pores of the FF, preventing effective filling of the storage. Detailed
235 analysis of varying precipitation intensities and durations reveals that C_{min} is getting much higher with prolonged rainfall events
236 2.2 g/g for a rainfall event lasting less than one hour up to mean C_{min} 2.6 g/g for very long events (> 10 h). For the intensity
237 data it becomes especially visible that for intensities higher 10mm/h the mean storage capacity drops down to 1.9 g/g. Likewise,
238 C_{max} is influenced by the duration of precipitation events. Here, the values are ranging from 2.3 g/g for events lasting less than
239 one hour to 2.8 g/g for events exceeding 10 hours. Also, the C_{max} values for events with an intensity higher than 10 mm/h are
240 much smaller with 2.1 g/g. All corresponding numbers can be found in Table 5.

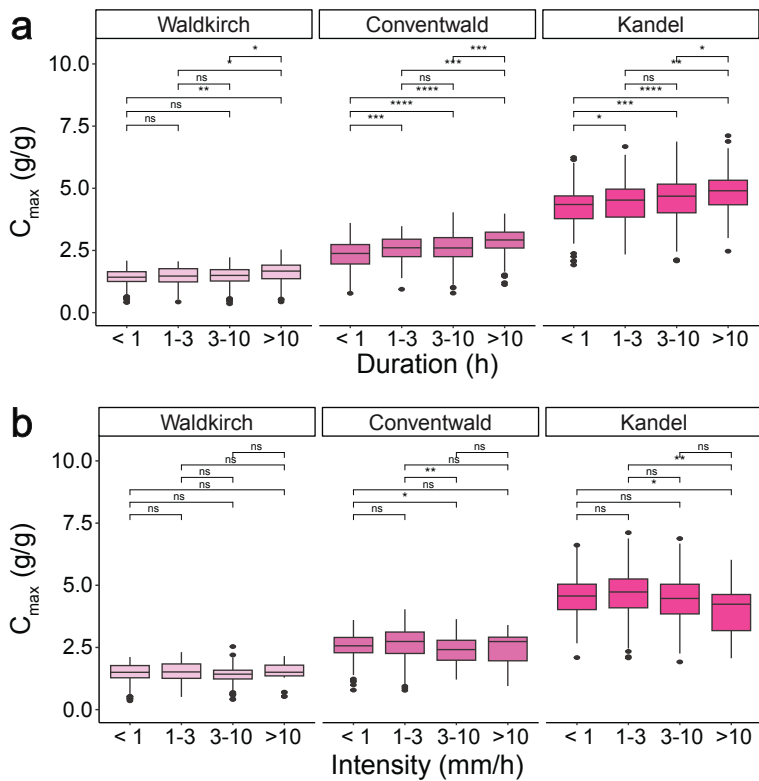


Figure 8: Mean interception capacity (C_{max}) on the three different research sites and for different precipitation durations (a) and consequently different precipitation intensities (b). Overlaid significance symbols indicate the results of statistical t-tests between the groups. The significance levels are represented as follows: * $(p \leq 0.05)$, ** $(p \leq 0.01)$, *** $(p \leq 0.001)$, **** $(p \leq 0.0001)$, and ns ($p > 0.05$).
 245



Table 5: Mean values and standard deviation (brackets) for C_{\min} and C_{\max} at the three different sites and for distinct precipitation durations and intensities.

	Mean C_{\min} (mm)	Mean C_{\max} (mm)	Mean C_{\min} (g/g)	Mean C_{\max} (g/g)
Location				
Waldkirch	28.3 (+/- 7.2)	29.9 (+/- 7.3)	1.4 (+/- 0.4)	1.5 (+/- 0.4)
Conventwald	23.2 (+/- 6.4)	24.8 (+/- 6.9)	2.4 (+/- 0.7)	2.6 (+/- 0.7)
Kandel	38.4 (+/- 7.0)	40.3 (+/- 7.4)	4.2 (+/- 0.8)	4.4 (+/- 0.8)
Duration				
< 1h	28.2 (+/- 9.2)	29.3 (+/- 9.1)	2.2 (+/- 0.7)	2.3 (+/- 0.7)
1 – 3 h	29.6 (+/- 9.1)	31.1 (+/- 9.4)	2.3 (+/- 0.7)	2.4 (+/- 0.7)
3 -10 h	29.6 (+/- 9.1)	31.3 (+/- 9.3)	2.2 (+/- 0.7)	2.3 (+/- 0.7)
> 10 h	32.3 (+/- 9.6)	35.2(+/- 10.2)	2.6 (+/- 0.8)	2.8 (+/- 0.8)
Intensity				
< 1 mm	30.2 (+/- 9.0)	31.5 (+/- 9.0)	2.2 (+/- 0.6)	2.3 (+/- 0.7)
1 – 3 mm	30.6 (+/- 9.8)	32.7(+/- 10.4)	2.5 (+/- 0.8)	2.7 (+/- 0.8)
3 -10 mm	28.6 (+/- 9.3)	30.4 (+/- 9.7)	2.3 (+/- 0.8)	2.5 (+/- 0.8)
> 10 mm	27.1 (+/- 8.2)	29.6 (+/- 8.5)	1.9 (+/- 0.6)	2.1 (+/- 0.6)

3.5. Evaporation

255 Evaporation on rain-free days, as shown in Figure 10 exhibits a pronounced diurnal pattern with a peak around midday. The highest evaporation rates (mm/h) occur at noon, coinciding with maximum temperatures and peak solar radiation. In Figure 9a we present the evaporation rates in Spring 2025 reaching up to 0.4 mm/h when the canopy is not yet fully developed, while during the depicted period in Summer 2024 with a fully closed canopy (Figure 9b), the maximum observed evaporation rate is only 0.16 mm/h. For both periods the soil moisture varied between 13 and 15 Vol-%, while the mean air temperature in
 260 spring was 15°C and in the depicted summer period was 20 °C

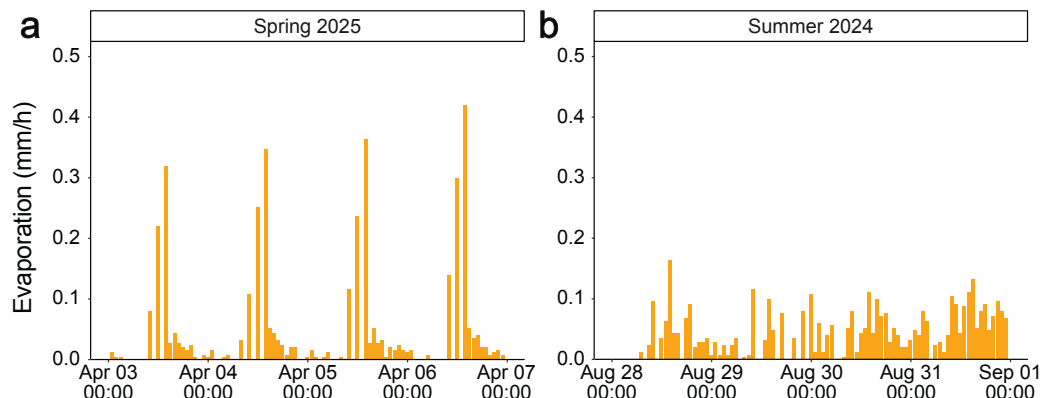


Figure 9: Diurnal pattern of evaporation fluxes from the FF for one exemplary timespan (28.08.2024-31.08.2024) and lysimeter (Spruce crown edge, Conventwald).

Average daily evaporation rates for days without rainfall range around 0.5 mm/d for the observed period. When examining 265 daily evaporation rates on rain-free days, it becomes apparent that daily evaporation rates do not differ significantly between the three research sites, but are highest at the Conventwald site, followed by Kandel, and Waldkirch. Due to the limited duration of rain-free periods (generally only a few days), overall daily evaporation rates do not differ substantially from first-day following precipitation evaporation, with mean values only slightly lower (Table 6).

270 **Table 6: Mean values and standard deviation (brackets) of evaporation rates for the three sites.**

Location	Evaporation (mm/d)	
	Days without rainfall	First day following rainfall
Waldkirch	0.51 (+/- 0.34)	0.53 (+/- 0.28)
Conventwald	0.54 (+/- 0.37)	0.58 (+/- 0.30)
Kandel	0.53 (+/- 0.29)	0.55 (+/- 0.32)

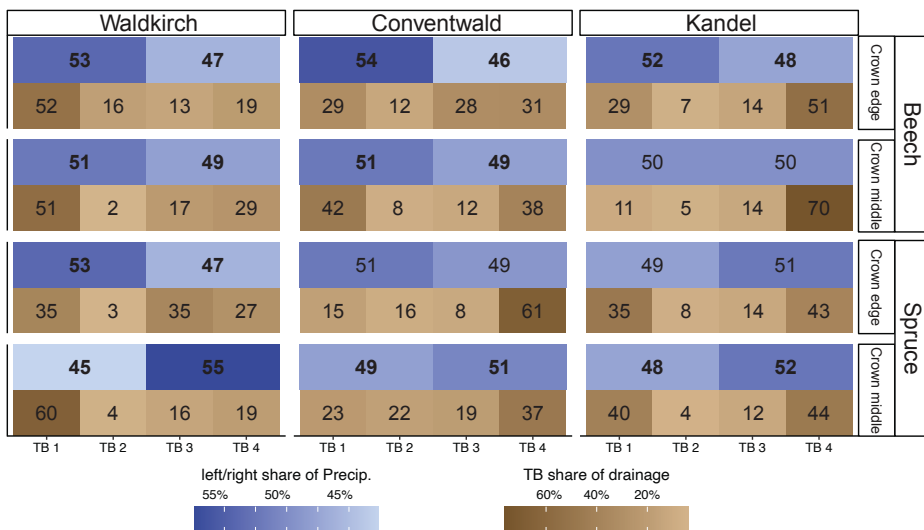
3.6. Infiltration distribution

The blue boxes in Figure 10 depict the average proportion of precipitation between the left and right sides for each of the 275 twelve lysimeters. In some cases, such as Kandel Beech crown middle, precipitation is equal proportioned (50/50%), whereas the most uneven proportion was observed in Waldkirch Spruce crown edge (45/55%). Statistical analysis revealed that in three quarters of the lysimeters (nine out of twelve), one side receives a significantly larger proportion of precipitation (bold numbers).



The brown boxes below illustrate the distribution patterns of percolating/draining water, divided among the four drainage grids of each lysimeter. The numbers represent the percentage share of total drainage at each grid location. Here, too, the degree of 280 distribution varies: some lysimeters, such as Conventwald Beech crown edge, exhibit relatively even distribution, while others, such as Kandel beech crown middle, show pronounced heterogeneity.

If the spatial patterns of precipitation and drainage are similar, we assume that there is minimal redistribution of precipitation water by the FF eg. Waldkirch Beech crown edge, where both precipitation and drainage are concentrated on the left side (primarily in TB1 and TB2). Conversely, if the patterns differ, we attribute this to redistribution processes by the FF and/or 285 the organic soil layer (eg. Waldkirch Spruce crown middle). For the majority of the twelve lysimeters, we observe diverging patterns in drainage distribution compared to precipitation input. This supports our hypothesis that the FF plays a critical role in redistributing incoming water, which may contribute to the development of preferential flow paths.



290 **Figure 10: Percentage share of precipitation (blue), bold numbers show a significant difference, and infiltration distribution (brown), showing the ability of the FF to redistribute water fluxes.**

4. Discussion:

4.1. Initial rainfall retention

Our findings support the hypothesis that a saturated FF lacks the capacity to retain additional water, whereas retention capability increases in drier conditions. The outliers observed in the "no retention" boxplots may be attributed to 295 hydrophobicity, which can occur under very dry conditions (Vogelmann et al., 2013). With hydrophobicity we assume that when the litter layer is very dry, its ability to retain water is significantly diminished, resulting in precipitation water rapidly



percolating through the layer without being retained. Unfortunately, 2024 was an unusually wet year, and we saw very few hydrophobic conditions during our field visits.

4.2. Storage capacity

300 Our findings show that sites with heavier FFs have higher water storage capacities, leading us to conclude that the ability to hold water is influenced by the proportion of organic fine material (OFM) rather than just a function of FF thickness. The range of observed water-holding capacity (C_{\min}) and interception capacity (C_{\max}) across our lysimeter network (Figure 7) can be attributed in part to our analytical approach. All precipitation events were analyzed without preconditioning the FF to a dry state, meaning storage was often not empty at the onset of an event. This methodological choice differs to most laboratory 305 studies, which typically being experiments on (oven-) dried material. In the natural environment, the litter layer is rarely, if ever, completely dry, and precipitation events frequently occur in rapid succession, preventing the full depletion of storage between them. This distinction complicates direct, quantitative comparisons with laboratory-derived values. For instance, (Sato et al., 2004) reported storage values of 0.44–1.74 g/g, while Putuhena and Cordery (1996) measured values around 1 g/g. The higher mean storage capacities observed in our study likely stem from the composition of our lysimeters, which were filled 310 not only with freshly fallen litter but also with fragmented FF material and the upper centimetres of the mineral soil (A horizon), resulting in a more complex, layered porous medium with greater overall water retention potential. As anticipated, the mean C_{\max} values were consistently higher than C_{\min} , as this metric includes gravitational water that drains rapidly following the cessation of rainfall (Putuhena and Cordery, 1996; Sato et al., 2004).

315 Aside from the intrinsic properties of the FF, our event-based field data show that storage capacity is also dynamically modulated by the specific characteristics of the precipitation event itself. We found that C_{\min} and C_{\max} are more effectively filled during prolonged, low-intensity rainfall events. This finding partly differs from previous research. Sato et al. (2004), for example, found that higher intensities were associated with greater storage, which could be attributed to the larger overall water volumes used in the controlled experiments. Similarly, our results contrast with those of Keim et al. (2006), who performed canopy irrigation experiments and found an increase in storage for canopy interception with rainfall intensity. The 320 most parsimonious explanation for these discrepancies is rooted in the difference between observational field studies and controlled laboratory simulations. Natural rainfall events with high intensity and long duration are uncommon in our study region. As a result, our field data, which reflects the actual distribution of storm events, is likely to underestimate these more extreme, high-volume events that can be easily created in the laboratory. Consequently, our results do not necessarily contradict previous work but rather provide a crucial real-world perspective, underscoring that the frequency and character of natural 325 rainfall are critical determinants of FF storage.

4.3. Evaporation

Examining daily evaporation rates on days without rain reveals that they are highest at the Conventwald site, followed by Kandel and Waldkirch, but do not differ significantly and are around 0.5 mm/d. Other studies, such as Magliano et al. (2017) align well with evaporation to be 1.1 ± 0.3 mm/day for forest litter at the first day after rainfall and Deguchi et al. (2008) with



330 seasonal variations in evaporation rates from the FF to be 0.2 ± 0.13 mm/day. The high spatial variability of their observation
was attributed to the local photo-environment of each sampling point, rather than to litter conditions, if the spatial variation in
air temperature or vapour pressure deficit at the FF is small relative to variation in radiation (Deguchi et al., 2008). The
differences of evaporation between our research sites could also be attributed to the larger water availability in the FF storage
at Conventwald, as discussed in the previous section. Additionally, differences in site exposure to wind and solar radiation are
335 likely to contribute to the observed patterns. Notably, despite Waldkirch being the warmest site, it has the lowest evaporation
rates, indicating that temperature is not the primary controlling factor for evaporation of the FF, but more the other factors
used in typical evaporation models (Penman-Monteith, (Beven, 1979)), like solar radiation, humidity or wind speed (Levia et
al., 2011). This is also evident when we look at the difference in diurnal pattern in spring and summer. Even though average
temperatures are higher in summer, we see higher hourly evaporation rates in spring due to higher solar radiation under the
340 less dense canopy. In general this diurnal pattern is consistent across all lysimeters and has also been described by Deguchi et
al. (2008), who reported midday peaks of approximately 0.04 mm per 30 minutes (equivalent to 0.08 mm/h), which aligns well
with our observations.

345 The differences in the pore size distribution between the FF and the underlying mineral soil can create a capillary barrier. This
capillary barrier effect has the potential to reduce the transport of water vapour from the mineral soil via FFs into the
atmosphere. As a result, the FF protects the mineral soil from evaporation. Our comparatively low evaporation rates suggest
that this protective function of the FF is present, just like Magliano et al. (2017) compared evaporation rates from FF
(1.1 mm/d), bare forest soil (4.4 mm/d) and pasture (7.0 mm/d). The effect of a protective function aligns also with the findings
of Florianic et al. (2022), who showed that the removing of the organic litter layer in a temperate mixed forest increased
evaporation from the underlying mineral soil.

350 **4.4. Infiltration**

The FF also influences water fluxes from the atmosphere into the mineral soil, as demonstrated by the water repellency of litter
surfaces (Greiffenhagen et al., 2006; Neris et al., 2013) or the low pore connectivity between the FF and the mineral soil. Water
repellency or low wettability is frequently observed in FFs at much higher residual water contents than in mineral soils
(Greiffenhagen et al., 2006; Wessolek et al., 2008). During dry periods, this water repellency potential increases significantly,
355 especially for thicker FF layers (Gimbel et al., 2016). The water repellency of FFs has been shown to increase overland flow
and runoff on inclined terrain (Neris et al., 2013) and alter infiltration dynamics and pathways (Gimbel et al., 2016; Orfánus
et al., 2021). Additionally, it may cause preferential flow along wettable microsites, directing rainwater predominantly towards
root surfaces (Wessolek et al., 2008). Our findings in Figure 11 provide a first insight to the redirection of water fluxes by the
FF at a small spatial scale, but further investigation is needed, particularly under dry and potentially hydrophobic conditions,
360 which we could not observe frequently enough in the period of study.



5. Conclusion

We present the results of a one-year forest floor grid lysimeter (FFGL) study conducted at three different sites and under two different tree species in the Black Forest, SW Germany. We continuously measured water fluxes into and from the FF, analysing 1,570 distinct precipitation events recorded by the 12 lysimeters situated across three beech-dominated forest sites
365 at varying altitudes. Our results show that the initial retention of precipitation water was not significantly affected by differences in FF thickness or mass, but rather by the pre-event water content of the FF. Although we observed initial indications of hydrophobic effects, the predominantly moist and wet conditions throughout the study period prevented us from detecting a significant hydrophobic influence on the retention capability of the FF. We found significant differences in storage capacities among the three sites, with greater FF mass and higher proportion of organic fine material (typical Moder at Kandel
370 and Conventwald) resulting in higher C_{min} and C_{max} values. However, precipitation characteristics had a significant impact on the observed storage dynamics. Low intensity, long-duration events facilitated more effective filling of the FF storage, whereas high-intensity, short-duration events resulted in lower storage values. The observed evaporation rates are consistent with previous. Due to the persistently wet conditions, we never observed complete drying of the FF storage, and the maximum duration of rain-free periods available for monitoring of evaporation was rather limited. The low evaporation rates indicate
375 that the FF works as a protective barrier against evaporation from the mineral soil. Our gridded lysimeter setup enabled us also to assess spatial water redistribution in the FF. Redistribution of incoming precipitation by the FF was evident in nearly all of the twelve lysimeters supporting the hypothesis that the FF plays an important role in modifying sub-surface hydrological pathways and infiltration processes in forests. Overall, our findings highlight the importance of FF properties especially FF mass and corresponding higher portions of organic fine material in controlling water storage, water retention, evaporation, and
380 the redistribution of precipitation in temperate forest ecosystems.

Acknowledgment

This project was carried out in the framework of Research Unit 5315 “Forest Floor: Functioning, Dynamics, and Vulnerability in a Changing World” funded by the Deutsche Forschungsgemeinschaft (DFG).

We would like to thank Florenz König for his technical support, Delon Wagner for his help in developing the electronical
385 setup of the lysimeters, and our student workers for their assistance in the field.

Code availability

The code used during the current study is available from the corresponding author on reasonable request.



Data availability

The datasets used and analysed during the current study are available from the corresponding author on reasonable request.

390 Author contribution:

MW and HP designed the setup. HP developed the lysimeter setup. HP wrote the first draft of the manuscript and performed data analysis. The manuscript was revised by MW and edited by HP.

Competing interests

There are no competing interests.

|395

References

AG Boden: Bodenkundliche Kartieranleitung, 6. Aufl. – Band 1: Grundlagen, Kennwerte und Methoden; Hannover, 2024.

Beven, K.: A sensitivity analysis of the Penman-Monteith actual evapotranspiration estimates, *J. Hydrol.*, 44, 169–190, [https://doi.org/10.1016/0022-1694\(79\)90130-6](https://doi.org/10.1016/0022-1694(79)90130-6), 1979.

400 Deguchi, A., Hattori, S., Daikoku, K., and Park, H.: Measurement of evaporation from the forest floor in a deciduous forest throughout the year using microlysimeter and closed-chamber systems, *Hydrol. Process.*, 22, 3712–3723, <https://doi.org/10.1002/hyp.6974>, 2008.

Florianic, M. G., Allen, S. T., Meier, R., Truniger, L., Kirchner, J. W., and Molnar, P.: Potential for significant precipitation cycling by forest-floor litter and deadwood, *Ecohydrology*, 16, <https://doi.org/10.1002/eco.2493>, 2023.

405 Gerrits, A. M. J., Savenije, H. H. G., Hoffmann, L., and Pfister, L.: New technique to measure forest floor interception – an application in a beech forest in Luxembourg, *Hydrol. Earth Syst. Sci.*, 11, 695–701, <https://doi.org/10.5194/hess-11-695-2007>, 2007.

Gimbel, K. F., Puhlmann, H., and Weiler, M.: Does drought alter hydrological functions in forest soils?, *Hydrol. Earth Syst. Sci.*, 20, 1301–1317, <https://doi.org/10.5194/hess-20-1301-2016>, 2016.

410 Greiffenhagen, A., Wessolek, G., Facklam, M., Renger, M., and Stoffregen, H.: Hydraulic functions and water repellency of forest floor horizons on sandy soils, *Geoderma*, 132, 182–195, <https://doi.org/10.1016/j.geoderma.2005.05.006>, 2006.

Guevara-Escobar, A., Gonzalez-Sosa, E., Ramos-Salinas, M., and Hernandez-Delgado, G. D.: Experimental analysis of drainage and water storage of litter layers, *Hydrol. Earth Syst. Sci.*, 2007.



Illek, A., Szostek, M., Mikołajczyk, A., and Rajtar, M.: Does Mixing Tree Species Affect Water Storage Capacity of the Forest Floor? Laboratory Test of Pine-Oak and Fir-Beech Litter Layers, *Forests*, 12, 1674, <https://doi.org/10.3390/f12121674>, 2021.

International Union of Soil Sciences (IUSS): World reference base for soil resources 2022: International soil classification system for naming soils and creating legends for soil maps, 4.edition., International Union of Soil Sciences, Vienna, Austria, 2022.

Keim, R. F., Skaugset, A. E., and Weiler, M.: Storage of water on vegetation under simulated rainfall of varying intensity, *Adv. Water Resour.*, 29, 974–986, <https://doi.org/10.1016/j.advwatres.2005.07.017>, 2006.

Levia, D. F., Carlyle-Moses, D., and Tanaka, T. (Eds.): *Forest Hydrology and Biogeochemistry: Synthesis of Past Research and Future Directions*, Springer Netherlands, Dordrecht, <https://doi.org/10.1007/978-94-007-1363-5>, 2011.

Li, Q., Lee, Y. E., and Im, S.: Characterizing the Interception Capacity of Floor Litter with Rainfall Simulation Experiments, *Water*, 12, 3145, <https://doi.org/10.3390/w12113145>, 2020.

425 Magliano, P. N., Giménez, R., Houspanossian, J., Páez, R. A., Nosetto, M. D., Fernández, R. J., and Jobbágy, E. G.: Litter is more effective than forest canopy reducing soil evaporation in Dry Chaco rangelands, *Ecohydrology*, 10, e1879, <https://doi.org/10.1002/eco.1879>, 2017.

Nanko, K., Keim, R. F., Hudson, S. A., and Levia, D. F.: Throughfall drop sizes suggest canopy flowpaths vary by phenophase, *J. Hydrol.*, 612, 128144, <https://doi.org/10.1016/j.jhydrol.2022.128144>, 2022.

430 Neris, J., Tejedor, M., Rodríguez, M., Fuentes, J., and Jiménez, C.: Effect of forest floor characteristics on water repellency, infiltration, runoff and soil loss in Andisols of Tenerife (Canary Islands, Spain), *CATENA*, 108, 50–57, <https://doi.org/10.1016/j.catena.2012.04.011>, 2013.

Orfánus, T., Zvala, A., Čierniková, M., Stojkovová, D., Nagy, V., and Dlapa, P.: Peculiarities of Infiltration Measurements in Water-Repellent Forest Soil, *Forests*, 12, 472, <https://doi.org/10.3390/f12040472>, 2021.

435 Paulsen, H. and Weiler, M.: Technical note: a Weighing Forest Floor Grid-Lysimeter, <https://doi.org/10.5194/egusphere-2024-3503>, 26 May 2025.

Pohl, S. and Garvelmann, J.: *SnoMoS Snow Monitoring Station Benutzerhandbuch*, 2015.

Putuhena, W. M. and Cordery, I.: Estimation of interception capacity of the forest floor, *J. Hydrol.*, 180, 283–299, [https://doi.org/10.1016/0022-1694\(95\)02883-8](https://doi.org/10.1016/0022-1694(95)02883-8), 1996.

440 Sato, Y., Kumagai, T., Kume, A., Otsuki, K., and Ogawa, S.: Experimental analysis of moisture dynamics of litter layers—the effects of rainfall conditions and leaf shapes, *Hydrol. Process.*, 18, 3007–3018, <https://doi.org/10.1002/hyp.5746>, 2004.

Van Stan, J. T., Coenders-Gerrits, M., Dibble, M., Boge Holz, P., and Norman, Z.: Effects of phenology and meteorological disturbance on litter rainfall interception for a *PINUS ELLIOTTII* stand in the Southeastern United States, *Hydrol. Process.*, 31, 3719–3728, <https://doi.org/10.1002/hyp.11292>, 2017.

445 Vogelmann, E. S., Reichert, J. M., Prevedello, J., Consenza, C. O. B., Oliveira, A. É., Awe, G. O., and Mataix-Solera, J.: Threshold water content beyond which hydrophobic soils become hydrophilic: The role of soil texture and organic matter content, *Geoderma*, 209–210, 177–187, <https://doi.org/10.1016/j.geoderma.2013.06.019>, 2013.



Walsh, R. P. D. and Voigt, P. J.: Vegetation Litter: An Underestimated Variable in Hydrology and Geomorphology, *J. Biogeogr.*, 4, 253, <https://doi.org/10.2307/3038060>, 1977.

450 Wessolek, G., Schwärzel, K., Greiffenhagen, A., and Stoffregen, H.: Percolation characteristics of a water-repellent sandy forest soil, *Eur. J. Soil Sci.*, 59, 14–23, <https://doi.org/10.1111/j.1365-2389.2007.00980.x>, 2008.

Zagyvai-Kiss, K. A., Kalicz, P., Szilágyi, J., and Gribovszki, Z.: On the specific water holding capacity of litter for three forest ecosystems in the eastern foothills of the Alps, *Agric. For. Meteorol.*, 278, 107656, <https://doi.org/10.1016/j.agrformet.2019.107656>, 2019.

455 Zhao, L., Meng, P., Zhang, J., Zhang, J., Sun, S., and He, C.: Effect of slopes on rainfall interception by leaf litter under simulated rainfall conditions, *Hydrol. Process.*, 36, e14659, <https://doi.org/10.1002/hyp.14659>, 2022.

460